

Studying Tuff Rings and Volcanic Hazards in a Tropical Setting: The Case of the Batoke Tuff Ring, Limbe, SW Region Cameroon

George Teke Mafany¹, Edison Forbuck Njei², Gerald G. J. Ernst^{3,4}, Wilson Yetoh Fantong¹,
Cheo Emmanue Suh², Samuel Ndonwi Ayonghe², Robert Stephen John Sparks⁵,
Koffi Teke Mafany², Stephen Manga Njome⁶

¹Institute of Geological and Mining Research, Yaoundé, Cameroon

²Department of Geology, University of Buea, Buea, Cameroon

³Department of Geology, University of Bamenda, Bamenda, Cameroon

⁴Department of Geology and Soil Science, University of Ghent, Ghent, Belgium

⁵Department of Earth Sciences, University of Bristol, Bristol, UK

⁶Department of Earth & Space/Physics, Cypress Springs High School, Houston, USA

Email: gmafany@yahoo.com

How to cite this paper: Mafany, G.T., Njei, E.F., Ernst, G.G.J., Fantong, W.Y., Suh, C.E., Ayonghe, S.N., Sparks, R.S.J., Mafany, K.T. and Njome, S.M. (2023) Studying Tuff Rings and Volcanic Hazards in a Tropical Setting: The Case of the Batoke Tuff Ring, Limbe, SW Region Cameroon. *Open Journal of Geology*, 13, 883-899.

<https://doi.org/10.4236/ojg.2023.138039>

Received: June 30, 2023

Accepted: August 27, 2023

Published: August 30, 2023

Copyright © 2023 by author(s) and Scientific Research Publishing Inc.

This work is licensed under the Creative Commons Attribution International License (CC BY 4.0).

<http://creativecommons.org/licenses/by/4.0/>



Open Access

Abstract

In subtropical volcanic environments, there are often few accessible outcrops. These are often highly weathered and of very poor quality. Soil development is rapid (1 cm/y) and small eruptions are unlikely to be preserved in the geological record. Reconstructing past eruptions and assessing hazards is a challenge. Here, we studied a poorly outcropping tuff ring (very poor, incomplete sections) with the best outcrop observed at a beach cliff (up to ca. 5 - 10 m high) at Batoke, to the south of Mt Cameroon volcano. Mt Cameroon has a few tuff rings, currently of unknown ages, near the SW coast of Cameroon. In the Batoke case, the sequence is dominated by gently dipping tuff beds varying in the proportion of lithics, juvenile clasts, and accretionary lapilli (acc-laps). Several beds are close-packed with acc-laps of up to 10 - 15 mm diameter. Part of the section is gullied by mud flow deposits. The rocks are highly weathered but differential weathering enhances relationships. Quantitative data can be extracted from a detailed study of outcrops' external surfaces. The preserved section is close to where the deposits were initially thickest and where acc-laps were most abundant and largest. There is an empirical correlation between maximum acc-lap size in the thickest outcrop and eruption column height. This and the deposit features suggest that the Batoke eruption was pulsating but dominated by fallout, with a water and ice-rich eruption column reaching 10 - 15 km high. Recycling of water drops and ice-coated fine ash accumulated during eruption. At switch off, wholesale gravitational collapse of this material produced the mud flows, which gullied the

previously-laid down deposits. Such ash fall and mud flows can represent a substantial hazard, e.g. they can gully down through towns and roads and cut evacuation routes. This study illustrates how, at subtropical tuff rings, it is possible to extract key data needed for hazard assessment from only 1 - 2 poor outcrops.

Keywords

Batoke Tuff Ring (BTR), Accretionary Lapilli

1. Introduction

The Batoke Tuff Ring (BTR) is found on the southern flank of the Mt Cameroon volcano (**Figure 1**).

Mt Cameroon is a large, 4095 m high stratovolcano that has erupted at least seven times in the past one hundred years. Workers (e.g. [1] [2] [3] [4]) who have attempted to assess the hazard potential of Mt Cameroon often rank the Hawaiian-style eruption that results in long lava flows, as the most common hazard. This is probably because lava flows are more recurrent as against the Strombolian to sub-plinian type eruptions that generate eruption columns and result in ash fall. Also, volcanic activity within the last 100 years has shown these explosive activities to be small and less frequent than lava flows. But for the 1959 eruption that did not follow the SW-NE fissure pattern [5], the TO READ when the explosive eruptions occur, they are invariably constrained along the corridor of these fissures [6]. This corridor coincides with the higher altitudes of the volcano that are relatively farther away from settlement. This has lent further credence to lava flows as the most important volcanic hazard in this region. Such an assertion is, however, illusory. From a geologic standpoint, 100 years of activity is not enough to draw overriding conclusions on the hazard potential of a volcano that is more than 1 M yr old. Small explosive activity today may become very violent large explosions tomorrow. Mt Krakatoa was dormant for 200 years before it erupted in 1883 in one of the most violent eruptions in history that resulted in the death of more than 36,000 people [7] [8] [9].

The few but extensive tuff rings like the BTR observed around the Mt Cameroon volcano are evidence that some unrecorded past eruptions were of strong explosive character. This has been confirmed in a study on the BTR that shows that it is of phreatomagmatic origin [10]. However, little is known about the eruption characteristics of these explosive eruptions because there has been no opportunity to effect real-time observations of such eruptions in this region. This is because they rarely occur. Information, therefore, has to be collected from deposits of past eruptions. This can be achieved by the study and observation of the tuff outcrops. Outcrop observation is, however, made difficult by the poor state of exposures in subtropical environments like that of Mt Cameroon—another aspect which has obscured the assessment of the hazard potential of explosive

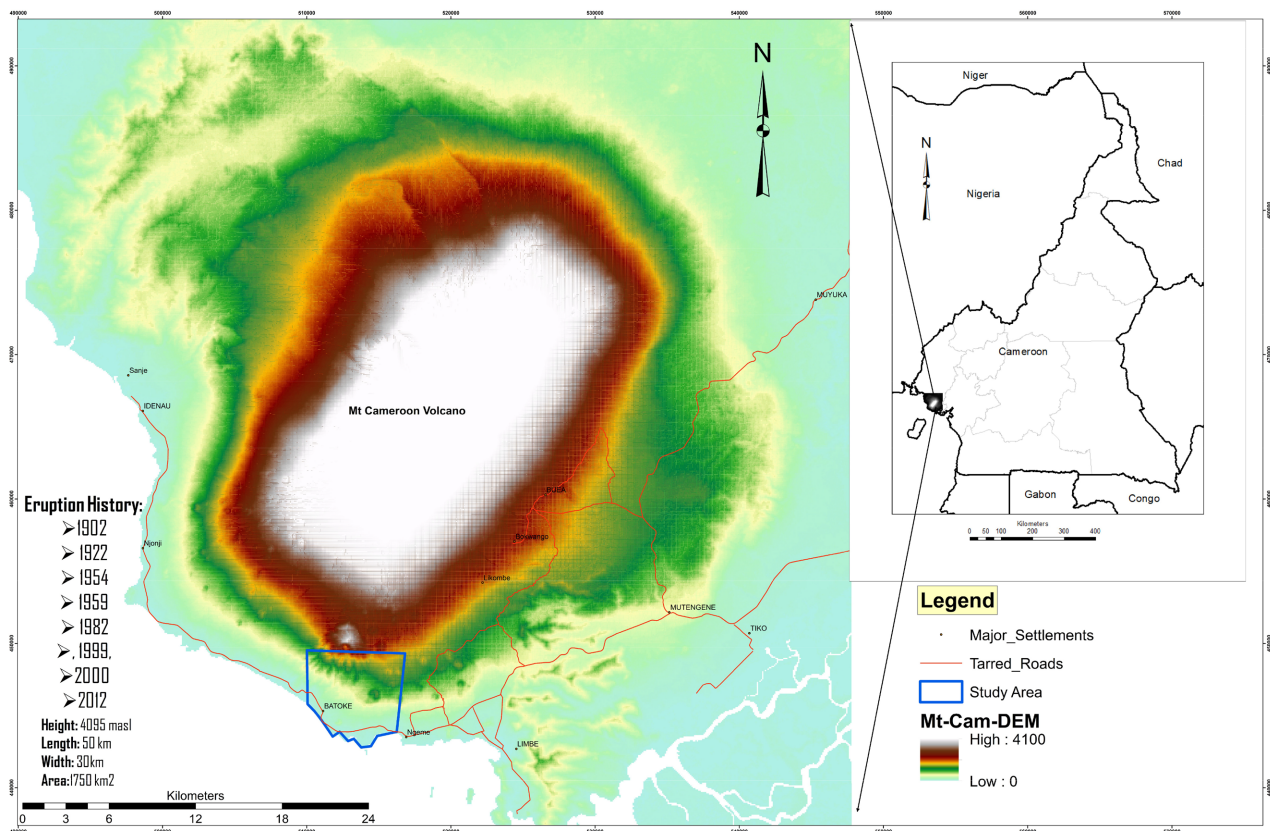


Figure 1. Digital elevation model of Mt Cameroon volcano showing location of the study area.

eruptions of Mt Cameroon. In subtropical volcanic environments, there are often few accessible outcrops. These are often highly weathered and of very poor quality. Soil development is rapid (1 cm/y) and small eruptions are unlikely to be preserved in the geological record. Reconstructing past eruptions and assessing hazards is, therefore, very difficult. The goal of this study is to demonstrate how invaluable data can be gleaned from the physical observation of a few outcrops and how such data can be used to reconstruct the eruption characteristics.

2. Field Investigations and Measurements

The BTR is one of the few tuff rings that has been preserved around Mt Cameroon and that contains records of past explosive eruptions of the volcano. It is found on the southern flank of the Mt Cameroon Volcano where it outcrops at several places including a cliff, and a road cutting with the best exposures found at the cliff. It is dissected by deep ravines some of which served in the past as lava flow channels. Its age is not yet known. It is, however, thought to be associated with early eruptions of Mt Cameroon more than 1 My old [1].

An attempt was made to map the spatial spread of the tuff ring based on field observation of outcrops backed by interpretation of satellite imagery (Figure 2).

It is quite extensive with a surface area of about 5 square kilometres (Figure 2). The thickest (about 10 m) observed portion is at the beach cliff outcrop from

where it extends northwards to terminate at Etinde village at the foot of the felspathoid Etinde massif some 4 km away.

The lone cone found in the vicinity of the tuff ring is suggested to be the source vent of the eruption. The 150 m high cone with a base of 0.3 km² was breached to the north; given its horse-shoe shape (Figure 3). This suggests that the ejecta was spewed northwards explaining why the bulk of the ash was deposited in this direction towards the Etinde Massif.

The tuff ring was logged at three different portions along the more than 200 m long and 10 m high coastal cliff exposure (Figure 4). The tuff beds dip gently from 10° in the NW to 30° in the SE such that from an accessibility standpoint it is easier to log the lower beds (Section A) in the NW, the upper beds (Section C) in the SE and the middle beds (Section B) somewhere between the NW and SE.

The three logs represent three different sets of beds which when superimposed from bottom to top in the order A, B, C give a more or less complete stratigraphic sequence (herein referred to as the detailed column) of the tuff ring cliff exposure (Figures 5(A)-(C)). The sections were investigated at millimetric scale with the aid of a hand lens only. Estimates were made of the relative proportions of accretionary lapillis, tuffaceous matrix and mafic particles present in each described layer. The sizes (the longest diameter) and core and rim thicknesses (where macroscopic measurements allowed) of the acc-laps were also measured. The colour and relative hardness of the various layers were determined.

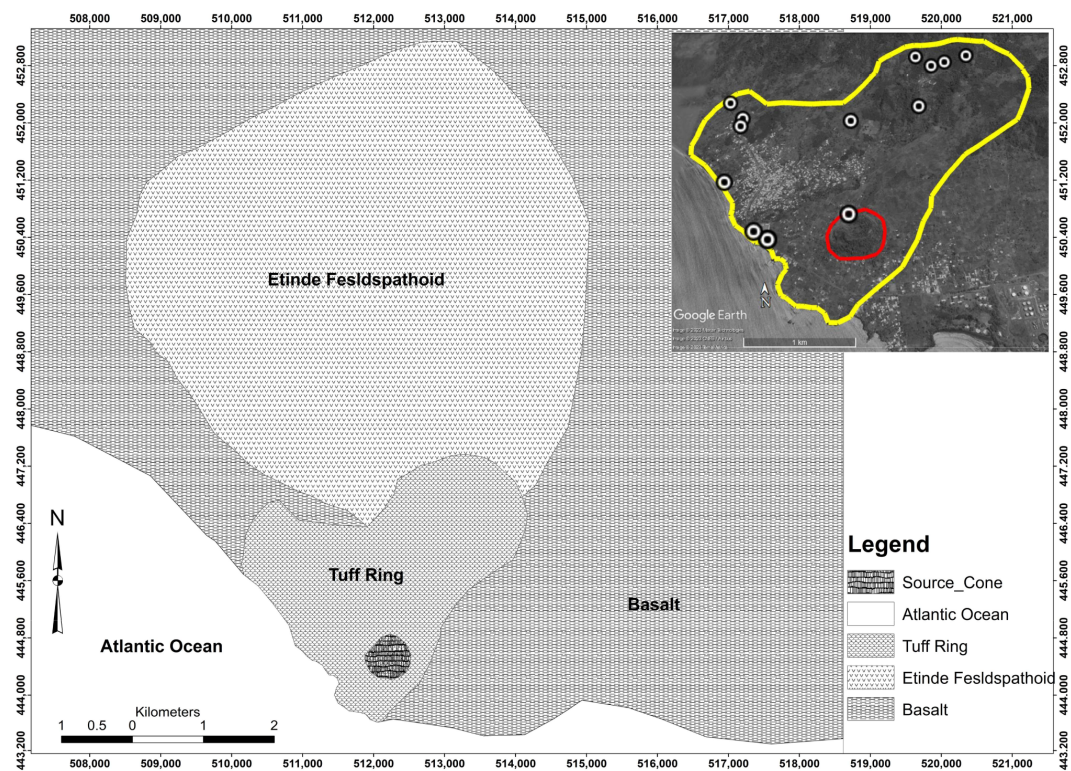


Figure 2. Geologic map of Batoke showing spatial extent of the Batoke Tuff Ring. Inset: Google earth 2021 landsat shows outcrop observation points (white dots) and source cone (red polygon) circumscribed by tuff ring (yellow polygon).

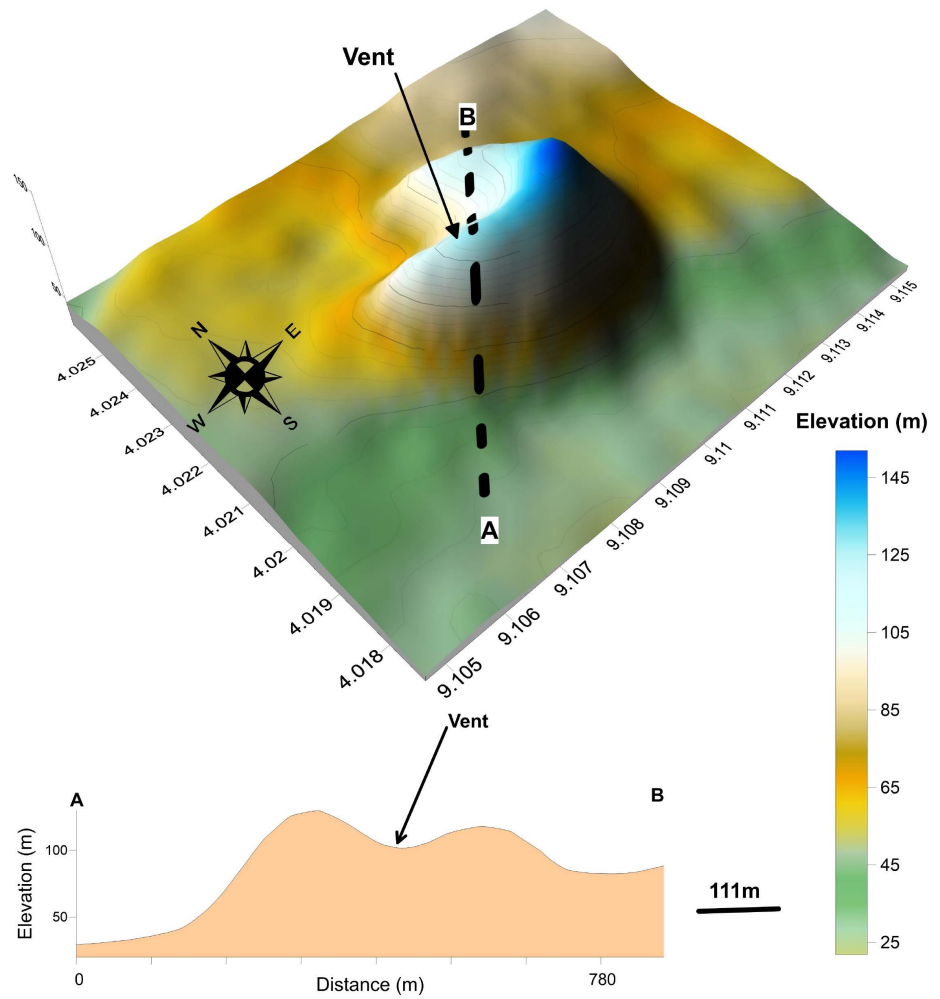


Figure 3. 3D model showing height and shape of the source cone of the eruption that resulted in the deposition of the Batoke Tuff Ring.

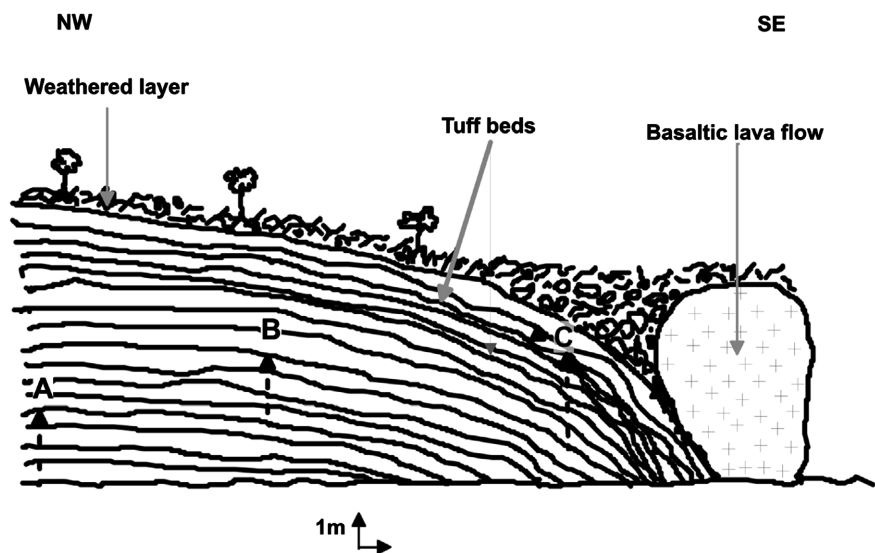


Figure 4. Schematic section of tuff ring exposure at Batoke Beach Cliff showing logged portions ((A) - (C)).

Depth (cm)	Thickness (cm)	Lithologic Description	AL Description	Modal Diameter of AL (mm)	% AL	% Tuff	% Mafic
0							
10	20	Indurated fine grained tuff	Well developed AL.	4	30	65	5
20	17	Friable coarse grained tuff	Well developed AL.	3	10	70	20
40	18	Fine grained tuff	Well developed AL.	4	35	60	10
50	7	Friable coarse grained tuff	Poorly developed AL.	5	85	10	
60	42	Scoriaeous lapilli. Scoria embedded in and supported by tuffaceous matrix. Scoria also occurs as load sags.	Poorly developed AL.	10	50	40	
70							
80	8	Friable coarse grained tuff	Poorly developed AL.	3	15	70	15
90	6	Indurated fine grained tuff	No AL.				
100							
110							
120							

(A)

Depth (cm)	Thickness (cm)	Lithologic Description	AL Description	Modal Diameter of AL (mm)	% AL	% Tuff	% Mafic
100							
120	23	Highly indurated very fine grained tuff	No AL.	none	0	95	5
140	10	Fine grained tuff	Poorly developed AL.	2	10	80	10
160	18	Indurated fine grained vesicular tuff	Well developed AL.	3	35	25	45
180							
200	67	Friable coarse grained tuff. Vesicular scoriaeous blocks embedded as load sags in tuff	No AL.	0	0	70	30
220							
240	6	Highly indurated very fine grained tuff	No AL.	0	0	85	15
260	19	Highly indurated tuff	Well developed AL.	5	45	50	5
280	12	Friable fine grained tuff	Poorly developed AL.	1	10	60	30
300	10	Fine grained friable tuff	Well developed AL.	5	10	80	10
320	15	Indurated fine grained tuff	Well developed AL.	3	35	60	5
340	14	Coarse grained tuff	Poorly developed AL.	1	10	75	15
360	16	Friable coarse grained tuff	No AL.	0	0	70	25
380	15	Coarse grained tuff	Poorly developed AL.	2	5	70	25
400	15	Coarse grained tuff	No AL.	0	0	90	10
420	29	Friable coarse grained tuff. Vesicular scoriaeous blocks embedded as load sags in tuff	No AL.	0	0	70	30
440	34	Indurated fine grained vesicular tuff	Well developed AL.	6	35	40	25
460	3	Highly indurated fine grained vesicular tuff	Well developed AL.	4	50	40	10
480	30	Indurated fine grained vesicular tuff	Well developed AL.	3	35	60	5

(B)

Depth (cm)	Thickness (cm)	Lithologic Description	AL Description	Modal Diameter of AL (mm)	% AL	% Tuff	% Mafic
460	4	Highly indurated very fine grained tuff	No AL.	0	0	80	20
	12	Fine grained tuff	Oblate AL.	8	35	60	5
480	10	Friable coarse grained tuff	Well developed AL.	3	15	70	15
	13	Loosely packed friable coarse grained tuff	Poorly developed AL. Aggregates form core of some AL.	3	10	60	30
500	20	Loosely packed friable coarse grained tuff	Well developed AL and aggregates. AL larger than 8 mm in diameter are oblate.	10	10	50	40
	3	Highly indurated tuff	Well developed AL.	7	25	75	0
520	5	Loosely packed friable coarse grained tuff	Well developed AL and aggregates. AL larger than 8 mm in diameter are oblate.	10	10	50	40
	10	Fine grained tuff	Poorly developed AL forming framework.	7	50	40	10
540	11	Coarse grained tuff	Well developed AL and aggregates. AL larger than 10 mm in diameter are oblate.	10	10	75	15
	11	Fine grained tuff	Well developed AL. Mafic particles observed in core of AL.	9	30	55	15
560	34	Coarse grained tuff	Poorly developed AL. Mafic with glassy particles.	3	15	70	15
	8	Fine grained tuff	Well developed AL.	4	25	60	15
580	9	Loosely packed friable coarse grained tuff	Poorly developed AL. Aggregates form core of some AL.	3	10	60	30
	26	Fine grained tuff	Well developed acc-laps. Mafic particles observed in core of acc-laps.	4	60	25	15
600	14	Indurated fine grained vesicular tuff	Well developed thick-rimmed AL.	2	25	60	15
	18	Coarse grained tuff	Poorly developed AL and aggregates.	8	30	40	30

(C)

Figure 5. Lithologic logs of the three different tuff sections studied at the Batoke Beach Cliff showing millimetric details of the tuff ring. AL = Accretionary Lapilli.

Based on grain size, presence or absence of acc-laps, quantity and type of acc-laps present, position of the layer/unit in the sequence and the response of each bed to weathering (differential weathering) the tuff ring was collapsed into thirteen main units to generate the collapsed column (**Figure 6**) described below from bottom to top.

A₁₅₋₁₃: The lowermost layer (A₁₅) of this lowermost unit is a friable coarse grained 18 cm thick tuff bed. It has poorly developed acc-laps which constitute ≈30% of total bulk volume. The acc-laps have a diameter range of 1 - 10 mm with 8 mm as the most recurring diameter. It is overlain by two layers 14 cm (A₁₄) and 26 cm (A₁₃) thick respectively. They are both highly indurated, fine grained tuff layers bearing well developed (distinct rim and core) acc-laps. However, A₁₄ is more vesicular, has smaller acc-laps (2 mm modal diameter) than the thicker A₁₃ whose abundant acc-laps (≈60%) peak at a diameter of 3 - 4 mm. Average rim thickness of acc-laps in A₁₄ is 1.5 mm. The rims are thicker than the cores. Mafic particles are clearly observed in the cores of A₁₃ acc-laps.

A₁₂: A scoriaceous lapilli unit separated from the lower unit by a distinct parallel boundary that in some places depresses down into the lower unit as a result of impact pits caused by huge scoria blocks (**Figure 3** see load sag). It is 12 cm

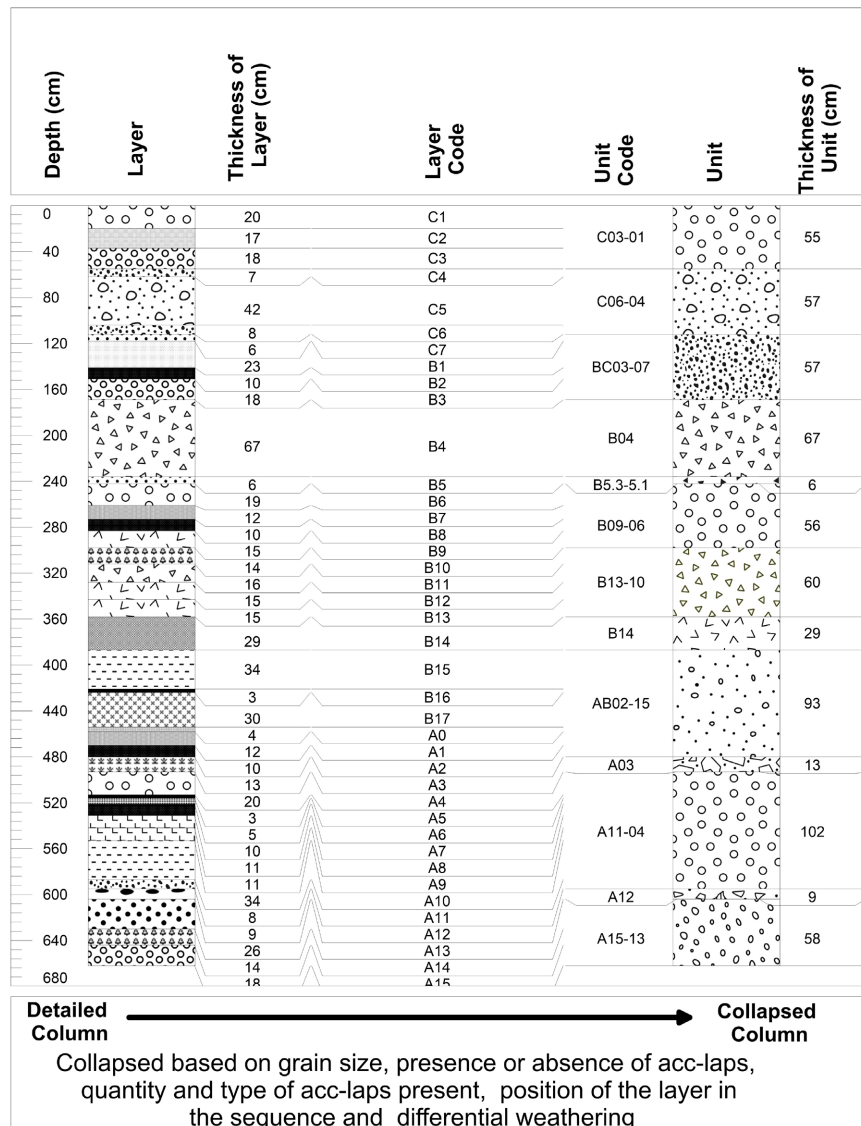


Figure 6. Lithologic logs showing the 40 logged layers (detailed column) collapsed into thirteen main units (collapsed column) based on grain size, presence or absence of acc-laps, quantity and type of acc-laps present, position of the layer in the sequence and differential weathering.

thick, poorly sorted and poor in acc-laps (<10%) which are very poorly developed.

A₁₁₋₀₄: This unit has eight layers which occur in an alternating sequence of highly indurated fine grained tuff and friable coarse grained tuff. The layers all contain well developed acc-laps although there is a dominance of poorly developed acc-laps in the coarse tuff. Besides its alternating layers, this unit is different from A₁₅₋₁₃ in that both the coarse grained and fine grained tuff of the unit have large diameter acc-laps up to 15 mm. Modal diameters of 8 mm are observed in the fine tuff. The coarse layers nonetheless have more abundant large and oblate acc-laps than the fine layers. The large acc-laps have fractured rims. Some of the fractures extend into the cores.

A₀₃: A₀₃ is similar to A₁₂ differing only in its greater thickness of 13 cm.

AB₀₂₋₁₅: Layer A₀₂ the bottom layer of this six-layered unit is the only coarse grained layer of the unit. It has no acc-laps and contains an abundance of mafic particles. The overlying 12 cm thick layer (A₀₁) is strongly indurated and rich in well developed and large acc-laps up to 10 mm in diameter. Acc-laps > 8 mm are spheroid. The next layer (A₀₀) in the sequence is just 4 cm thick. It is indurated, vesiculated and has no acc-laps. The thickness increases to 30 cm in the layer above (B₁₇) which is also indurated and vesiculated but is rich in acc-laps (35%). The acc-laps have a maximum diameter of 6 mm and a modal range of 3 - 4 mm. B₁₆ is similar to the preceding layer except that the acc-laps constitute 50% of the total bulk volume of the layer and it is just 3 cm thick. B₁₅ the uppermost and thickest (34 cm) layer of the unit is also indurated and rich in acc-laps (35%) but the acc-laps are smaller (2 mm) than in all the other layers.

B₁₄: B₁₄ is a scoriaceous 29 cm thick, coarse grained lapilli tuff unit. Scoria blocks attain diameters of 24 cm. It is similar in most aspects to A₁₂ and A₀₃ but has no acc-laps.

B₁₃₋₁₀: All the four layers of this unit are coarse grained friable tuff. Each has a mean thickness of ≈15 cm. The first, (B₁₃) has no acc-laps. It is overlain by B₁₂ that contains a few poorly developed acc-laps. The pattern repeats itself in the next two layers.

B₀₉₋₀₆: This unit begins with an indurated fine grained layer (B₀₉ – 15 cm) rich in well-developed acc-laps. It is followed by an equally fine grained but friable and acc-laps-poor (10%) - though well-developed - layer (B₀₈ – 10 cm). The subsequent layer (B₀₇ – 12 cm) is also friable, fine grained and acc-laps poor (10%). But the few acc-laps are poorly developed. Finally the topmost layer (B₀₆) is thicker (19 cm) and richer (45%) in well developed acc-laps averaging 4 mm in diameter.

B_{5.3-5.1}: Three layers of equal thickness (2 cm each) with one coarse grained and friable and the other two fine grained and indurated characterise this unit. The coarse grained layer is sandwiched between the two indurated fine grained layers. All the layers are devoid of acc-laps.

B₀₄: B₄ is very similar to A₁₂ and A₀₃. Nonetheless it is the thickest (67 cm) scoriaceous unit of the entire sequence and has no acc-laps.

BC₀₃₋₀₇: BC₀₃₋₀₇ begins from the bottom with an indurated fine grained vesicular 10 cm thick layer (B₀₃) rich in well developed acc-laps (35%). The modal range of acc-laps is 2 - 3 mm with maximum diameters of 10 mm observed. The sequence continues onto the next layer (B₀₂) with fine grained tuff but no vesicles and few (10%) and poorly developed acc-laps. B₀₂ is also 10 cm thick. The acc-laps deficiency accentuates in the overlying highly indurated fine grained layer (B₀₁) where there are no acc-laps at all. It is 23 cm thick. The topmost layer (C₀₇) of the unit is similar to B₀₁ though slightly less indurated.

C₀₆₋₀₄: C₀₆ (8 cm thick) and C₀₄ (7 cm thick) are similar as they are both friable, coarse grained and are poor in acc-laps which are largely poorly developed. C₀₅, a scoria bearing lapilli tuff layer is sandwiched between them. It is 42 cm thick

and has scoria blocks as large as 16 cm. The scoria is embedded in and supported by the tuffaceous matrix. The scoria also occurs as load sags and contains some poorly developed acc-laps.

C₀₃₋₀₁: C₀₃₋₀₁ is typified by three layers all containing well developed acc-laps. The 17 cm thick coarse grained middle layer (C₀₂) has fewer acc-laps (10%) as against 35% and 30% for C₀₃ and C₀₁ respectively. C₀₂ is sandwiched between C₀₃ (18 cm thick) and C₀₁ (20 cm thick) _{both} indurated fine grained tuff layers. The mean diameter of the acc-laps is 3 mm.

From the foregoing, the BTR is characterised by an alternating sequence of fine grained tuff and coarse grained tuff layers. The scoria occurs in some places as load sags. Both the fine grained and coarse grained tuffaceous layers contain accretionary lapillis. Some of the tuff horizons (irrespective of grain size) are vesiculated. However, the quantity and type of acc-laps vary with the type of layer.

The fine grained tuff layers invariably contain acc-laps. The acc-laps are smaller with a diameter range of 2 - 5 mm. They are in most cases well developed with well defined cores and rims and a sharp grain size break between the core and the rim. In some of these fine grained layers the acc-laps are so abundant (up to 60% bulk volume) that they form the framework of the layer.

Many of the coarse grained layers do not contain acc-laps and when the acc-laps are present they are usually few and are matrix supported. These coarse grained layers contain from the smallest (<1 mm) to the largest acc-laps (20 mm) dominated by the 10 - 13 mm range. The smaller acc-laps (<1 mm) manifest poorly developed characteristics.

In both the fine and coarse grained layers, the small acc-laps are spherical while the large ones are oblate. The rims of the oblate acc-laps usually have fractures which sometimes extend into their cores. Both poorly developed and well developed acc-laps are common to both types of layers but the former is more common in the coarse tuff than in the fine tuff which is typified by the latter. The cores of all the acc-laps (small or large, spherical or oblate) are vesiculated and have coarser particles than the rims. There is no clear relationship between the thickness of the layer and grain size or acc-laps content.

3. Interpretations and Discussions

The eruption characteristics, height of eruption column and emplacement model are interpreted from the physical attributes of the tuff ring described above.

3.1. Eruption Characteristics

New data generated during this study on the extensive nature of the BTR (more than 5 km²), the abundance of well developed acc-laps, the absence of rootless and/or spatter cones but presence of cinder cone in the vicinity of the tuff ring and whose northerly breaching direction coincides with the direction of abundance of the ash fall deposit posits that the eruption was caused by the interac-

tion between a rising magma source and surface water and not by simple interaction between an advancing lava and surface water source as suggested by [10]. For well developed acc-laps to form they need an abundant supply of fine ash, rain and an ash cloud sufficiently high or sufficiently dense [11]. Low content of fine ash and inadequate cloud height usually less than 100 m [12] typical of littoral rootless cone eruptions cannot generate the acc-laps observed in the Batoke Tuff Ring. Furthermore, the classic line of evidence for a littoral rootless cone, namely the occurrence of two partcones on either side of a lava corridor, with synchronicity of the part-cones and lava [11] and the presence of spatter cones [12] is not available in Batoke. Only the remnant of one cinder cone is visible.

The BTR eruption ring was dominated by sub-areal phreatomagmatic activity with occasional switches to Strombolian activity. Change in eruption style occurred when the cone grew above the water level to exclude further influence of water. The occurrence of Strombolian activity is evidenced by the thick scoriaceous units observed in the sequence and around the source vent of the eruption. The alternation between coarse and fine grained beds suggests that the eruption was rapidly pulsating and was characterised by an alternation of vigorous and weak explosions. But for the occasional breaks marked by the presence of scoriaceous units, the change in acc-laps size and type and the subtle changes in average grain size and/or the proportion of lithic clasts, the BTR sequence is monotonous. This suggests that the time between the pulsating explosions was short. This time is a function of the rate at which magma and water converged at the vent [13] and which in the Batoke case is suggested to be high.

The eruption that resulted in the emplacement of the BTR was of phreatomagmatic origin as already established by [10]. Surface water was the main source of water. Groundwater-driven sub-surface explosions are consistent with abundance of accidental debris derived from underlying strata [14] and such eruptions usually result in maars and not tuff rings [15]. We use the fact that the studied pyroclasts are tuff rings, the near absence of accidental debris in the tuff and the proximity of the tuff ring to the Atlantic Ocean which had been there before the onset of the first eruption of Mt Cameroon to infer that the provenance of the water was from a surface water source and not groundwater. The abundant acc-laps and vesiculation of most layers is further evidence that large amounts of water participated in this eruption [16] and such large amounts could only be supplied by an external source like surface water. More credence to this assertion is supplied by experimental studies carried out by [17] who have demonstrated that for tuff rings to form, a magma/water ratio of 1:1 is required. Such a low ratio is invariably furnished by a large surface water body which in this case could be seawater.

The presence of distinct scoriaceous units and bomb sags in some tuff layers implies deposition took place within the range of ballistically dispersed pyroclast. The parallel to sub-parallel bedding is evidence that the layers were deposited beyond the limits of any constructional features such as tuff cones or rings developed around source vents [14]. [18] has shown that the presence of vesicu-

lated horizons suggest that tuff have been deposited with abundant water and are the product of very wet co-surge fall out. The vesicles are attributed to thawing, partly during fall and partly after deposition [19] and to the coalescence of damp acc-laps after rapid deposition [20]. [13] interprets strongly indurated tuff as wet surge deposits and poorly indurated, thinly bedded tuff as dry-surge deposits. We recognise the hard indurated vesiculated fine grained tuff layers of the Batoke sequence as products of wet surges while the friable layers are of dry surge origin. The presence of acc-laps and the absence of undulatory bedding, low angle cross stratification, climbing dune forms and so on (features characteristic of base surges) indicate that both the fine grained and coarse grained planar-bedded layers of the Batoke tuff are primarily of airfall origin.

3.2. Accretionary Lapillis and Their Implications

Accretionary lapillis may be formed by volcanic eruptions or meteorite impact events [21]. However, the single, sub-spherical, regularly-shaped rim structure of acc-laps observed in the BTR suggests they are of volcanic origin compared against the multiple or irregularly shaped rims of meteorite impact-related aggregates. Volcano-related acc-laps are formed in wet hydrovolcanic or phreatomagmatic eruptions in which water ejected directly from the vent or condensed from steam [14] or supplied by rain that falls through the ash [22] results in the nucleation of ice on ash particles in the ash cloud [18]. This causes cohesion of the ash particles [23]. Cohesion is accentuated by electrostatic attraction in the ash cloud [22] [24] [25]. The result is the non-selective aggregation of both fine and coarse ash particles. The maximum diameter of these aggregates is limited by “drop break-up” to 5 - 6 mm and accretion of ash is attenuated at 5 - 6 km asl by freezing of the aggregates at a temperature of about -13°C [18]. The acc-laps that exceed this diameter-range are formed by further growth of aggregates that remain longer in suspension and at higher altitudes (6 - 9 km asl) as a result of re-entrainment or recycling. At about 4 km asl on their way down, the aggregates start to thaw from the outside. The resulting thin film of liquid water at the rim, favours the size-selective accretion of fines as the acc-laps fall through elutriated ash layers [26] or through secondary co-surge intrusions [18] to form well-developed acc-laps. We intimate that the small acc-laps observed in the BTR were formed at 5 - 6 km asl while the large ones formed at 10 - 15 km asl. This implies that the eruption was violent enough to project material to such heights given it a surteseyan character as observed by [27] [28]. An eruption of such magnitude will pose serious threats to aircraft aviation and riparian populations.

Contrary to the close association of acc-laps and fine vesiculated ash observed by [18] for the Santorini tuff, the Batoke tuff exhibits a co-existence of small acc-laps (<6 mm in diameter) and fine grained tuff (vesiculated or not) on one hand and large acc-laps (>6 mm) and coarse grained ash on the other hand. This is consistent with a simultaneous emplacement of fine ash and small acc-laps on one hand and coarse ash and large acc-laps on the other hand. Fine ash and small

acc-laps generally have smaller terminal velocities than coarse ash and large acc-laps. It would, therefore, be expected that the coarse ash and large acc-laps would be emplaced first before the fine ash and small acc-laps. The alternation of these layers in the Batoke sequence and the non-exposure of the lowermost layer (in contact with the country rock) make it difficult to determine the chronology of deposition. We, however, postulate that, an initial water-rich explosion produced an ash-laden plume that rose several kilometres asl. Due to the difference in terminal fall velocities between the coarse ash and fines in the ash plume, gravitational forces caused the rapid fall-out of the former [24] without allowing enough time for the formation of acc-laps. This is thought to account for the acc-laps-free coarse grained tuff layers (e.g. B₁₃).

The fines that remain in suspension and at higher altitudes favour the formation of acc-laps. Agglomeration of fine ash increases their terminal fall velocities and causes a simultaneous sedimentation of acc-laps and fine ash, hence their co-existence in the same tuff layers. During fall-out, few ($\approx 10\%$) of these acc-laps are recycled or re-entrained to higher heights [18] resulting in further growth of the acc-laps to attain diameters above 6 mm. These larger acc-laps are sustained in suspension by the buoyancy effect produced by the latent heat released by freezing of the acc-laps [18]. All these take place as plume activity progressively dwindles from its initial vigour. Without a complete attenuation of the eruption, another vigorous pulse is released, injecting more coarse material into the eruption column. This increases the gravitational forces and causes the coarse ash to pull down the large acc-laps out of suspension resulting in a coeval sedimentation of both.

Class II volcanic fragments classified in terms of dispersal behaviour [27] [28] dominate the material involved in acc-laps formation. These fragments have terminal fall velocities that are substantially smaller than the velocities of the turbulence inside the umbrella cloud but greater than the velocities of the turbulence of the atmosphere outside the cloud [27] [28] factors which are favourable from a buoyancy and re-entrainment stand point for the formation of acc-laps.

Poorly developed acc-laps are also known to be closely associated with coarse grained layers some of which bear large well-developed acc-laps. These aggregates do not develop distinct cores and rims because they are either precipitously or rapidly removed from suspension by settling coarse ash introduced into the plume by a vigorous pulse or melting doesn't commence until they are deposited. Their co-existence with large well-developed acc-laps in a coarse matrix underpins the possibility that the coarse material rises to 10 - 15 km asl where it triggers the settling of the large acc-laps and as the mixture continues its downward trend, it incorporates the poorly developed acc-laps at lower altitudes (<6 km asl). Rimming in poorly developed acc-laps is hampered either because the settling rate is so fast that it doesn't allow the size-selective accretion of fines at the outer margin of the aggregates or the aggregates do not melt until they are deposited.

The deep gullies dissecting the BTR were formed at the end of the eruption. At the stop of the eruption, most of the suspended material falls back around the vent [18]. As it falls, most of the ice thaws and this results in short-lived torrential showers of high intensity. These showers perpetrate flash floods that dissect the already deposited material to produce deep gullies.

3.3. Hazard Implications

Recent eruptive activity (past 100 years) of Mt Cameroon is confined to fissure-controlled vents running NE-SW [29]. But for the remnants of some cones found on the southwestern flank of the volcano that are proximal to the Atlantic Ocean, most of the recent vents are distal from any significant surface water bodies. As a result, the occurrence of an explosive, surface water-driven phreatomagmatic eruption like that which deposited the BTR may be erroneously considered to be unlikely around the Mt Cameroon Volcano. The absence of surface water in the fissure zone where vents are most likely to open up does not preclude the incidence of a phreatomagmatic eruption because this corridor hosts significant quantities of groundwater that may cause an explosive hydrovolcanic eruption. That the 1959 eruption did not respect the SW-NE fissure pattern [5] is also proof that an eruption can break out anywhere on the edifice at a place that may harbour sufficient water to replicate the BTR eruption.

Ephemeral lakes are formed when water collects in large depressions dammed by lava flows or in volcanogenic craters on a volcano [30]. Abundant rainfall of above 3000 mm per annum (that climaxes to above 9000 mm per annum on the southwestern flank in Desbunscha) and a morphology typified by depressions and more than 100 cinder cones provide for the occurrence of ephemeral lakes on Mt Cameroon volcano. Such water bodies may fortuitously serve as sources that may trigger volcano-hydrologic hazards as was observed during the 2000 eruption of Mt Cameroon where a small short-lived phreatic eruption (lasted less than 2 mins) that produced a plume height of about 30 m broke out on the lava front that was advancing towards Bokwaongo. No casualties to life and property were observed firstly because it was small and secondly because it took place in the forest zone away from human settlement.

There is also a high possibility of lava flowing into the Atlantic Ocean as almost happened in the 1999 eruption in Bakingili where the flow stopped less than 200 m from the ocean. This could generate a littoral eruption with the attendant ash fallout.

The BTR has not yet been completely mapped, so it is possible that it may be more extensive than has been described in this study. Should such an extensive ash fall occur again it will pose a huge threat to human life and property.

4. Conclusions

The BTR had never been described in such detail before. In this study, we use the BTR to show how, at subtropical tuff rings, it is possible to extract key data

needed for hazard assessment from only 1 - 2 poor outcrops through physical observation of the outcrops. We also illustrate that ash fall is an important volcanic hazard in the Mt Cameroon region.

This investigation has demonstrated that:

1) The eruption was caused by the interaction between a rising magma source and surface water and not by simple interaction between an advancing lava flow and a surface water source.

2) The eruption was pulsating but energetic enough to result in an ash plume that rose to more than 10 km as to allow for the formation of well-developed acc-laps.

3) Upon switch-off of the eruption, the gravitationally unstable base of the umbrella cloud orchestrated a catastrophic fall-out of ash and frozen aggregates. This resulted in the rapid and massive deposition of tuffs and intense torrential rains that caused flash floods. These flash floods incised deep gullies in the already laid down deposits.

4) Such an eruption represents a serious hazard to aircraft and riparian populations around the volcano.

Funding

Partial financial support for this work was obtained through a grant awarded by the International Association of Sedimentology (IAS) to G. T. Mafany.

Conflicts of Interest

The authors declare no conflicts of interest regarding the publication of this paper.

References

- [1] Deruelle, B., N'ni, J. and Kambou, R. (1987) Mount Cameroon: An Active Volcano of the Cameroon Line. *Journal of African Earth Sciences*, **6**, 197-214. [https://doi.org/10.1016/0899-5362\(87\)90061-3](https://doi.org/10.1016/0899-5362(87)90061-3)
- [2] Njome, S., Suh, C.E., Chuyong, G. and De Wit, M.J. (2010) Volcanic Risk Perception in Rural Communities along the Slopes of Mount Cameroon, West-Central Africa. *Journal of African Earth Sciences*, **58**, 608-622. <https://doi.org/10.1016/j.jafrearsci.2010.08.007>
- [3] Wantim, M., Jacobs, P., Suh, E., Kervyn, M. and Ernst, G. (2012) Mapping and Modelling Lava Flow Dynamics and Hazards at Mount Cameroon Volcano. *Afrika Focus*, **25**, 101-102. <https://doi.org/10.21825/af.v25i1.18063>
- [4] Del Marmol, M.A., Fontijn, K., Atanga, M., Njome, S., Mafany, G., Tening, A., Wantim, M.N., Fonge, B., Che, V.B., Aka, F., Ernst, G.G.J., Suh, E., Jacobs, P. and Kervyn, M. (2017) Investigating the Management of Geological Hazards and Risks in the Mt Cameroon Area Using Focus Group Discussions. In: Fearnley, C.J., *et al.*, Eds., *Observing the Volcano World: Volcano Crisis Communication*, Springer, Berlin, 373-394. https://doi.org/10.1007/11157_2017_3
- [5] Njome, M.S., Suh, C.E., Sparks, R.S.J., Ayonghe, S.N. and Fitton, J.G. (2008) The Mount Cameroon 1959 Compound Lava Flow Field: Morphology, Petrography and

- Geochemistry. *Swiss Journal of Geosciences*, **10**, 85-98.
<https://doi.org/10.1007/s00015-007-1245-x>
- [6] Suh, C.E., Sparks, R.S.J., Fitton, J.G., Ayonghe, S.N., Annen, C., Nana, R. and Luckman, A. (2003) The 1999 and 2000 Eruptions of Mount Cameroon: Eruption Behaviour and Petrochemistry of Lava. *Bulletin of Volcanology*, **65**, 267-281.
<https://doi.org/10.1007/s00445-002-0257-7>
- [7] Dolgoff, A. (1996) *Physical Geology*. Heath and Company, Lexington.
- [8] Brata, A.G., Rietveld, P., De Groot, H.L.F. and Zant, W. (2013) The Krakatau Eruption in 1883: Its Implications for the Spatial Distribution of Population in Java. *Economic History of Developing Regions*, **28**, 27-55.
<https://doi.org/10.1080/20780389.2013.866381>
- [9] Abdurrachman, M., Widiyantoro, S., Priadi, B. and Ismail, T. (2018) Geochemistry and Structure of Krakatoa Volcano in the Sunda Strait, Indonesia. *Geosciences*, **8**, Article 111. <https://doi.org/10.3390/geosciences8040111>
- [10] Ngwa, C.N., Nche, L. and Suh, C.E. (2013) Physical Volcanology of Pyroclastic Tephra Deposit at Batoke Mt. Cameroon, West Africa: An Overview. *Global Journal of Geological Science*, **11**, 27-35. <https://doi.org/10.4314/gjgs.v11i1.3>
- [11] Walker, G.P.L. (1992) Puu Mahana near South Point in Hawaii Is a Primary Surtseyan Ash Ring, Not a Sandhills-Type Littoral Cone! *Pacific Science*, **46**, 1-10.
- [12] Mattox, T.N. and Mangan, M.T. (1997) Littoral Hydrovolcanic Explosions: A Case Study of Lava-Seawater Interaction at Kilauea Volcano. *Journal of Volcanology and Geothermal Research*, **75**, 1-17. [https://doi.org/10.1016/S0377-0273\(96\)00048-0](https://doi.org/10.1016/S0377-0273(96)00048-0)
- [13] Aranda-Gomez, J.J. and Luhr, J.F. (1996) Origin of the Joya Honda maar, San Luis Potosi, Mexico. *Journal of Volcanology and Geothermal Research*, **74**, 1-18.
[https://doi.org/10.1016/S0377-0273\(96\)00044-3](https://doi.org/10.1016/S0377-0273(96)00044-3)
- [14] Hanson, R.E. and Elliot, D.H. (1996) Rift-Related Jurassic Basaltic Phreatomagmatic Volcanism in the Central Transantarctic Mountains: Precursory Stage to Flood Basalt Effusion. *Bulletin of Volcanology*, **58**, 327-347.
<https://doi.org/10.1007/s004450050143>
- [15] Lorenz, V. (1986) On the Growth of Maars and Diatremes and Its Relevance to the Formation of Tuff Rings. *Bulletin of Volcanology*, **48**, 265-274.
<https://doi.org/10.1007/BF01081755>
- [16] Lorenz, V. (1974) Vesiculated Tuffs and Associated Features. *Sedimentology*, **21**, 273-291. <https://doi.org/10.1111/j.1365-3091.1974.tb02059.x>
- [17] Wohletz, K.H. and McQueen, R.G. (1984) Experimental Studies of Hydromagmatic Volcanism. In: *Explosive Volcanism: Inception, Evolution, and Hazards*, National Academy Press, Washington DC, 158-169.
- [18] Go, S.Y. and Sohn, Y.K. (2021) Microtextural Evidence for Vesiculated Tuff Formation in Songaksan Tuff Ring, Jeju Island, Korea. *Journal of Volcanology and Geothermal Research*, **417**, Article ID: 107311.
<https://doi.org/10.1016/j.jvolgeores.2021.107311>
- [19] Giaiotti, D., Gianesini, E. and Stel, F. (2001) Hueristic Considerations Pertaining Hailstone Size Distributions in the Plain of Friuli-Venezia Giulia. *Atmospheric Research*, **57**, 269-288. [https://doi.org/10.1016/S0169-8095\(01\)00080-1](https://doi.org/10.1016/S0169-8095(01)00080-1)
- [20] Rosi, M. (1992) A Model for the Formation of Vesiculated Tuff by the Coalescence of Accretionary Lapilli. *Bulletin of Volcanology*, **54**, 429-434.
<https://doi.org/10.1007/BF00312323>
- [21] Mueller, S.B., Kueppers, U., Huber, M.S., Hess, K.U., Poesges, G., Ruthensteiner, B.

- and Dingwell, D.B. (2018) Aggregation in Particle Rich Environments: A Textural Study of Examples from Volcanic Eruptions, Meteorite Impacts, and Fluidized Bed Processing *Bulletin of Volcanology*, **80**, Article No. 32. <https://doi.org/10.1007/s00445-018-1207-3>
- [22] Schumacher, R. and Schmincke, H.U. (1991) Internal Structure and Occurrence of Accretionary Lapilli: A Case Study at Laacher See Volcano. *Bulletin of Volcanology*, **53**, 612-634. <https://doi.org/10.1007/BF00493689>
- [23] Brown, R.J., Branney, M.J., Maher, C. and Dávila-Harris, P. (2010) Origin of Accretionary Lapilli within Ground-Hugging Density Currents: Evidence from Pyroclastic Couplets on Tenerife. *Geological Society of America Bulletin*, **122**, 305-320. <https://doi.org/10.1130/B26449.1>
- [24] Lane, S.J. and Gilbert, J.S. (1992) Electric Potential Gradient Changes during Explosive Activity at Sakurajima Volcano, Japan. *Bulletin of Volcanology*, **54**, 590-594. <https://doi.org/10.1007/BF00569942>
- [25] Miura, T., Koyaguchi, T. and Tanaka, Y. (2001) Measurements of Electric Charge Distribution in Volcanic Plumes at Sakurajima Volcano, Japan. *Bulletin of Volcanology*, **64**, 75-93. <https://doi.org/10.1007/s00445-001-0182-1>
- [26] Alvarado, G.E. and Soto, G.J. (2002) Pyroclastic Flow Generated by Crater-Wall Collapse and Outpouring of the Lava Pool of Arenal Volcano, Costa Rica. *Bulletin of Volcanology*, **63**, 557-568. <https://doi.org/10.1007/s00445-001-0179-9>
- [27] Koyaguchi, T. and Ohno, M. (2001) Reconstruction of Eruption Column Dynamics on the Basis of Grain Size of Tephra Fall Deposits: 1. Methods. *Journal of Geophysical Research*, **106**, 6499-6512. <https://doi.org/10.1029/2000JB900426>
- [28] Koyaguchi, T. and Ohno, M. (2001) Reconstruction of Eruption Column Dynamics on the Basis of Grain Size of Tephra Fall Deposits: 2. Application to the Pinatubo 1991 Eruption. *Journal of Geophysical Research*, **106**, 6513-6533. <https://doi.org/10.1029/2000JB900427>
- [29] Suh, C.E., Ayonghe, S.N. and Njumbe, E.S. (2001) Neotectonic Earth Movements Related to the 1999 Eruption of Cameroon Mountain, West Africa. *Episodes*, **24**, 9-12.
- [30] Manville, V., Hodgson, K.A. and Nairn, I.A. (2007) A Review of Breakout Floods from Volcanogenic Lakes in New Zealand. *New Zealand Journal of Geology and Geophysics*, **50**, 131-150.